Developmental Cell, Volume *23*

Supplemental Information

An RNAi Screen Reveals Intestinal Regulators of Branching Morphogenesis, Differentiation, and Stem Cell Proliferation in Planarians

David J. Forsthoefel, Noëlle P. James, David J. Escobar, Joel M. Stary, Ana P. Vieira, Forrest A. Waters, and Phillip A. Newmark

INVENTORY OF SUPPLEMENTAL INFORMATION

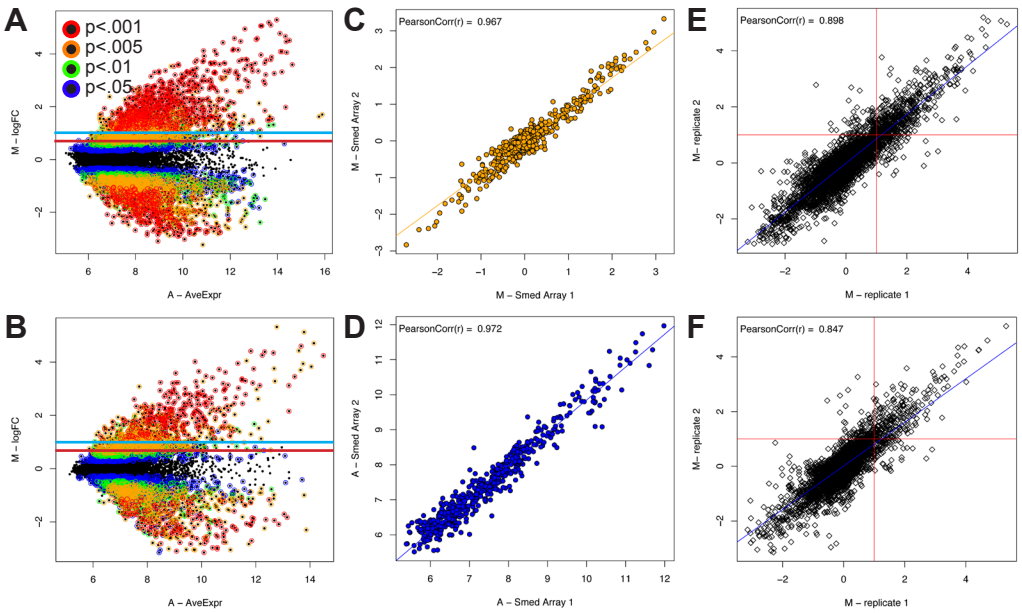

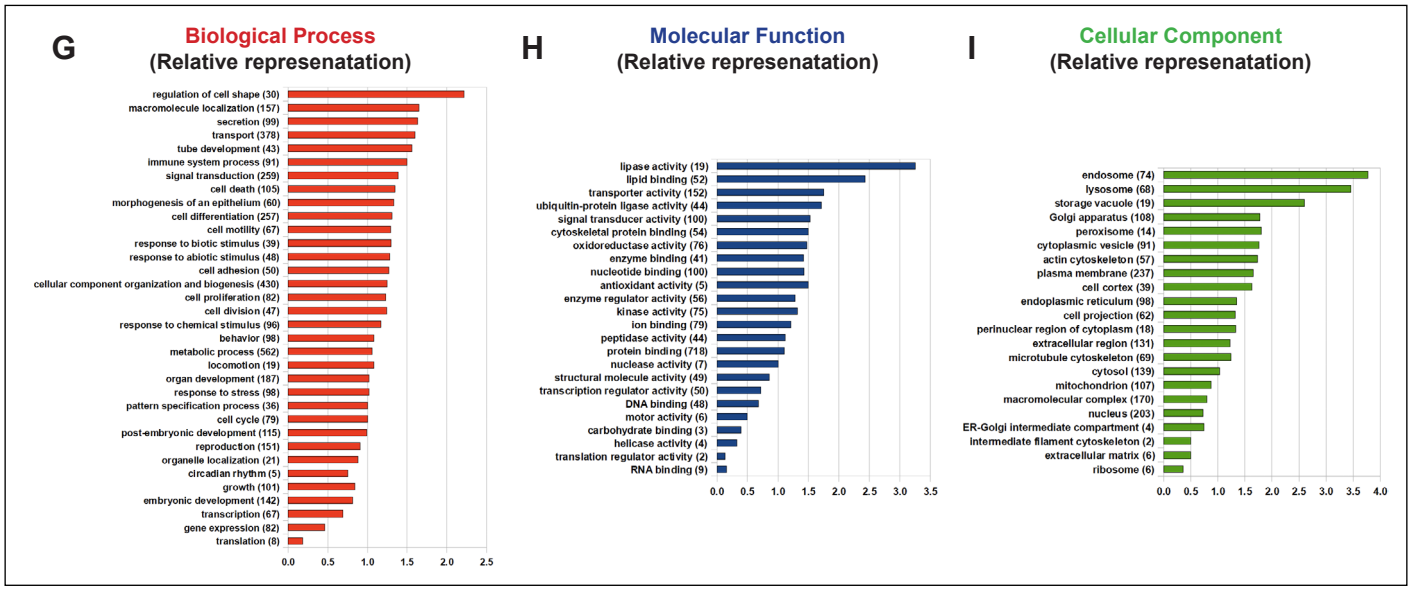

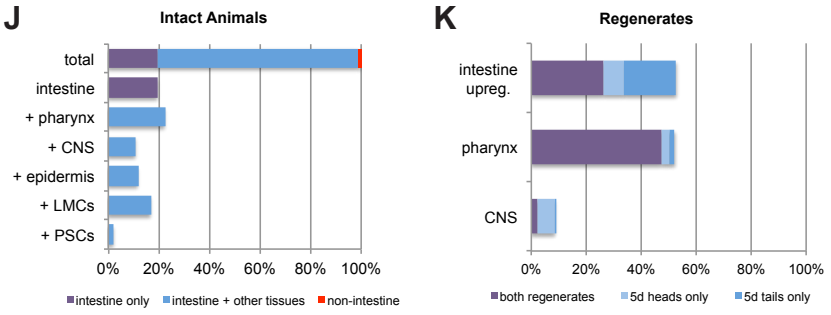

Figure S1, Related to Figure 2.

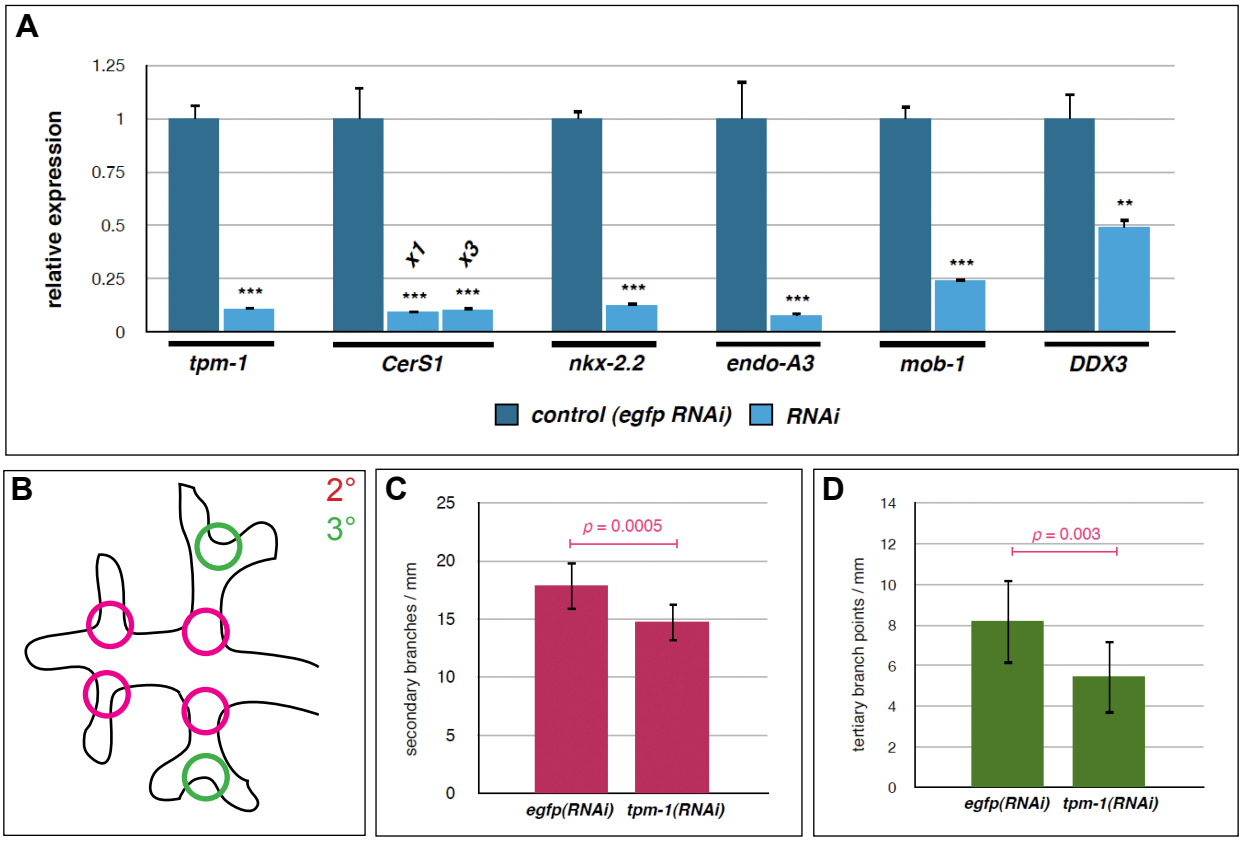

Figure S2, Related to Figure 3.

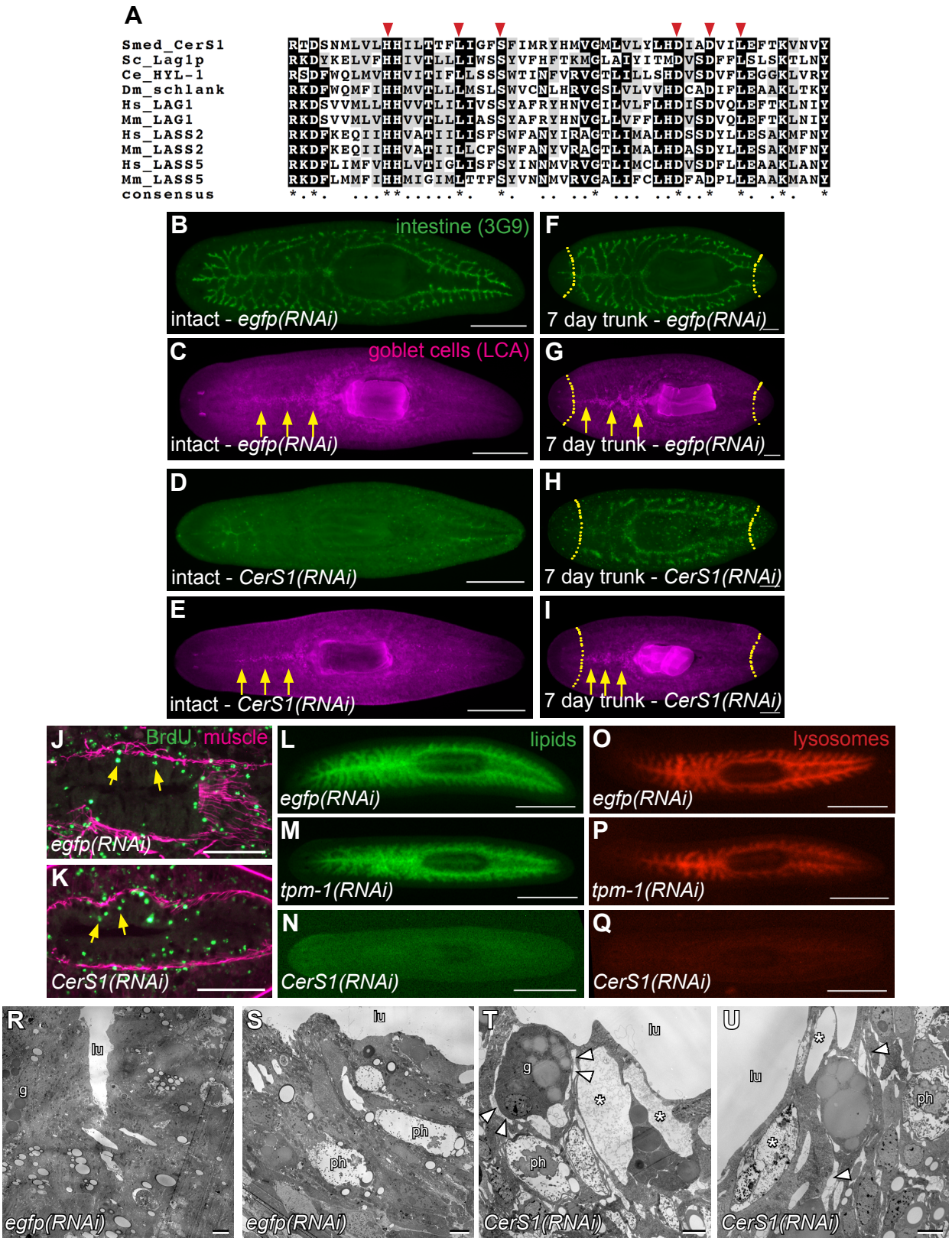

Figure S3, Related to Figure 4.

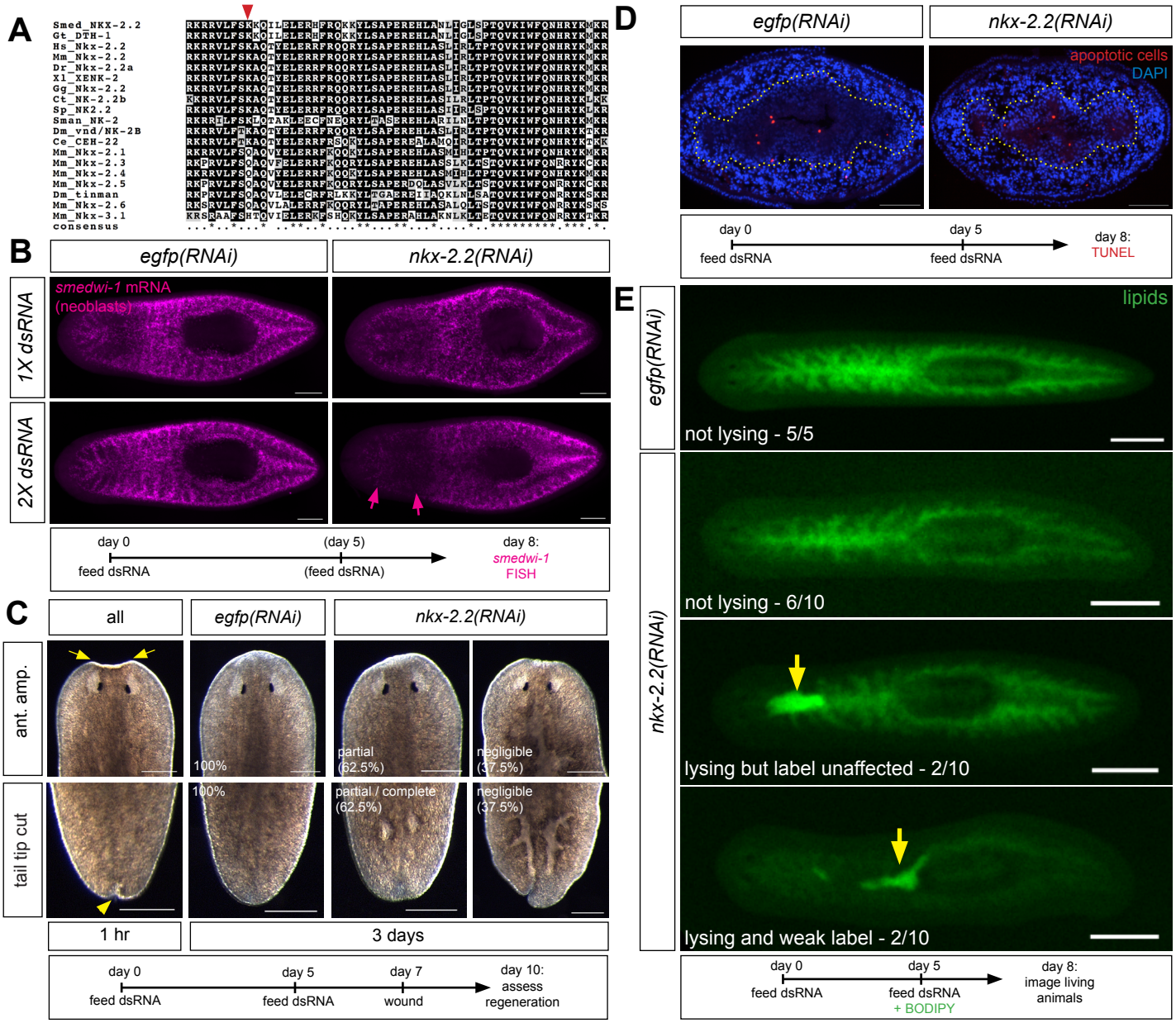

Figure S4, Related to Figure 6.

Supplemental Figure Legends

Figure S1. 1514 transcripts are upregulated in intestinal phagocytes, Related to Figure 2. (A and B) “MA” (ratio-intensity) plots showing normalized expression values for 11,521 transcripts represented on two separate oligonucleotide arrays. Average overall expression level for individual probes on the array (A value) is represented on the X axis (i.e., higher is to the right), while differential expression (M value) is plotted on the Y axis; all values are $\log_2$-transformed. Adjusted *p*-values for individual probes are shown by colored circles. Transcripts upregulated 2-fold or greater (M>1, 1841 probes representing 1081 genes) are located above the blue horizontal line; an additional 434 genes are upregulated between 1.5-fold (M=0.6) and 2-fold, between red and blue horizontal lines. (C and D) Correlation plots between arrays. Normalized M values (C) or A values (D) for oligonucleotide probes duplicated on both arrays were plotted against each other on X (array 1 or “SmedArray1”) or Y (array 2 or “SmedArray2”) axes to visualize the correlation between arrays for the same labeled aRNA samples, demonstrating the reproducibility of hybridizations conducted in parallel. Pearson correlation coefficients (*r*) are indicated at the top left of each plot. Regression lines are indicated in orange (C) or blue (D).(E and F) Correlation plots within arrays. Within-array correlation for transcripts represented by two distinct probes on the first (“SmedArray1”, E) and second (“SmedArray2”, F) arrays. Pearson correlation coefficients (*r*) are indicated at the top left of each plot. Regression lines are indicated in blue (E and F). M values of 1 are represented by red horizontal and vertical lines in E and F. (G-I) Representation of gene ontology categories in the transcriptome of intestinal phagocytes. The percentage of 1514 intestine-specific genes with each annotation was divided by the percentage of all 11,521 genes on the arrays with each annotation to determine relative under- (less than 1.0) or over-representation (over 1.0) as a ratio,

shown on the X-axis. Terms with the greatest representation are located at the top of each plot. The number of genes to which each term was assigned in the intestinal phagocyte transcriptome is indicated in parentheses. (J, K) Histograms showing the percentage of genes (n=218) expressed in various tissues in intact (J) and regenerating (K) animals. LMCs, lateral marginal cells; PSCs, peripharyngeal secretory cells.

Figure S2. Quantitative PCR validation of dsRNA-mediated knockdown and quantification of *tropomyosin-1(RNAi)* branching morphogenesis defects, Related to Figure 3. (A) Quantification of relative transcript levels after RNAi. Animals were fed dsRNA-expressing bacteria two or three times (see Supplemental Methods), or, in the case of *CerS1,* either once (x1) or three times (x3) (indicated). In most cases transcripts decreased >75% after knockdown. *tpm-1, CerS1,* and *nkx-2.2* knockdown caused phenotypes, while knockdown of *endo-A3, mob-1,* and *DDX3* did not. Results are the average of three biological replicates (individual planarians). Error bars, standard deviation; ***, $p<0.001$; **, $p<0.005$, Student's *t*-test. (B-D) Quantification of reduction in intestinal branches in *tpm-1(RNAi)* animals. After five dsRNA feedings, animals were fixed and labeled with MAb 3G9. Secondary and tertiary branch points were counted as in (B), expressed as a ratio to overall animal length in mm, and averaged (n=12 animals each). *tpm-1(RNAi)* animals possessed ~18% fewer secondary branches (C) and ~33% fewer tertiary/quaternary branches (D). Error bars, standard deviation; *p*, Student's *t*-test.

Figure S3. *Smed-CerS1* is required for differentiation of functional intestinal phagocytes, Related to Figure 4. (A) Alignment of the Lag1 motifs of various Lass family members. Amino acids essential for Lag1 catalytic activity (Spassieva et al., 2006) are conserved in *Smed-CerS1* (red arrowheads). Identical residues are shaded in black; consensus residues (>60% similarity of aligned sequences) are shaded in gray. Because the *S. mediterranea* genome contains a second *CerS* gene encoding a Lag1p motif in which

not all catalytically essential amino acids are conserved (not shown), and which is not preferentially expressed in the intestine (Contig2561, Table S1), we refer to the gene encoded by Contig2269 as *CerS1.* (Smed, *Schmidtea mediterranea;* Sc, *Saccharomyces cerevisiae;* Ce, *Caenorhabditis elegans;* Dm, *Drosophila melanogaster;* Hs, *Homo sapiens;* Mm, *Mus musculus).* (B-E) Differentiation of LCA-labeled goblet cells (magenta, arrows in C and E, mainly in primary branches) is unaltered after *CerS1* knockdown, even though 3G9 labeling (green, B vs. D) is almost completely lost. Feeding regimen was identical to Fig. 4D-E. (F-I) *CerS1* knockdown also does not lead to preferential differentiation of LCA-labeled goblet cells during regeneration (magenta, arrows in G and I). Feeding regimen was identical to Fig. 4F-K. (J-K) BrdU-positive enterocytes (arrows, luminal side of the enteric muscle boundary) are born at similar rates in control (J) and *CerS1(RNAi)* (K) animals (4 day chase). At 12-24h, only neoblasts label with BrdU (not shown) (Forsthoefel et al., 2011). dsRNA feeding was conducted as in Figure 4D-E, except that BrdU was fed to animals instead of dsRNA-expressing bacteria for the fourth feeding. Animals were fixed 4 days after feeding. (L-Q) *CerS1* is required for intestinal cells to retain lipid (N) and lysosome (Q) markers. Animals were fed as in Fig. 4L-N. (R-U) Electron micrographs of the intestines of control (R and S) and *CerS1(RNAi)* (T and U) animals 10 days after three dsRNA feedings. lu, lumen. g, goblet cell. ph, autophagosome. Asterisks, large intercellular gaps. Arrowheads, regions where lateral cell:cell contacts appear to be disrupted. Epifluorescent images of immunolabeled samples (B-I), cryosections (J and K), and living animals (L-Q). Anterior is to the left in B-I and L-Q; dorsal is up in J and K. Scale bars: 500 μm (B-E); 200 μm (F-I); 100 μm (J-K); 1 mm (L-Q); 3 μm (R-U).

Figure S4. NKX-2.2 homeodomain alignment, and further characterization of *Smed-nkx-2.2* phenotypes and *nkx-2.2* expression, Related to Figure 6. (A) Alignment of

homeodomains from *Smed*-NKX-2.2 and other representative NK-class transcription factors. *Smed*-NKX-2.2 is most similar to vertebrate and invertebrate Nkx-2.2 orthologs, based on reciprocal TBLASTN analyses. In particular, *Smed*-NKX-2.2 shares a lysine residue (red arrowhead) that is not conserved in other NK homeodomains. (Smed, *Schmidtea mediterranea;* Gt, *Girardia tigrina;* Hs, *Homo sapiens;* Mm, *Mus musculus;* Dr, *Danio rerio;* Xl, *Xenopus laevis;* Gg, *Gallus gallus;* Ct, *Capitella teleta;* Sp, *Strongylocentrotus purpuratus*; Sman, *Schistosoma mansoni;* Dm, *Drosophila melanogaster;* Ce, *Caenorhabditis elegans*). (B) After two dsRNA feedings, *nkx-2.2* knockdown results in partial loss of *smedwi-1*-positive neoblasts in the anterior third of the animal (arrows) (*smedwi-1* FISH). Images are representative of at least three specimens for each condition. (C) Some *nkx-2.2(RNAi)* animals partially regenerate after minor injury. Three days after wounding, 62.5% (n=16 for each condition) of *nkx-2.2(RNAi)* animals produce small anterior blastemas after amputation of the tip of the head (yellow arrows). Similarly, 62.5% of *nkx-2.2* knockdown animals partially or completely regenerate after incision of the tail tip (yellow arrowhead). n=16 animals per condition. By three days after injury, 11/16 (~69%) of *nkx-2.2(RNAi)* anterior amputation animals had begun to lyse; 14/16 (~88%) of tail tip poke animals were lysing. (D) *nkx-2.2* does not lead to increased apoptosis in the intestine (yellow dotted line) or elsewhere. Apoptotic cells were visualized via TUNEL assay on 20 μm cryosections from the anterior (prepharyngeal) region. Images are representative of sections from at least three animals per condition; 3-5 sections were analyzed per animal. (E) Most *nkx-2.2(RNAi)* animals retain a lipid binding dye, including some that have begun to lyse (yellow arrows, 2/10 animals). (F) *nkx-2.2*-positive cells (as well as *hnf4*-positive cells) (arrowheads) are detectable in the mesenchymal space between posterior intestinal branches three days after gamma irradiation; *smedwi-1*-positive cells are ablated. Maximal projections of five confocal sections per panel (~5 μm total thickness). Anterior

is to the left in B and E, and to the top in C and F; dorsal is to the top in B. Scale bars: 200 μm (B); 250 μm (C); 100 μm (D); 500 μm (E); 50 μm, insets 5 μm (F).

Supplemental Experimental Procedures

RNA isolation, amplification, and labeling

Intestinal cells (2-5 x 10^5) and ~10% of non-intestinal cells (1-3 x 10^6) from 100 large asexual planarians were lysed in 1 mL Trizol (Invitrogen), and total RNA (typically 1-4 μg) was isolated according to the manufacturer's instructions, using the high-salt step for RNA precipitation. RNA was DNAse-treated, purified, and concentrated using the DNA-free RNA kit (Zymo Research). 500 ng of total RNA were amplified using the Amino Allyl MessageAmp II aRNA Amplification Kit (Ambion). ~12 μg labeled aRNA were coupled to Alexa Fluor 555 or Alexa Fluor 647 succinimidyl ester dyes (Molecular Probes) according to the MessageAmp II protocol, followed by column purification using either Ambion's Labeled aRNA filter Cartridges or Zymo's RNA Clean & Concentrator-5 kit.

Microarray design, hybridization, and analysis

35- to 40-mer oligonucleotide probes were designed complementary to 11,521 planarian transcripts, the majority of which represented expressed sequence tag (EST) "contigs" and individual unassembled ESTs ((Zayas et al., 2005) and http://newmark13.life.illinois.edu/est/cgi-bin/login.cgi). In most cases, two unique oligos were designed per transcript. Probes were synthesized on two individual CombiMatrix "CustomArray" oligonucleotide arrays (Table S1; Figure S1). Most transcripts were represented on only one array, however, ~300 were duplicated on both arrays, enabling correlation of differential expression values and overall expression levels between arrays

(Figure S1). Labeled aRNA targets were hydrolyzed with RNA Fragmentation Reagent (Ambion/Applied Biosystems), hybridized to arrays following CombiMatrix protocols, and imaged using a GenePix 4000B Scanner and GenePix Pro 6.0 software (Axon Instruments/Molecular Devices). Four independent biological replicates were conducted with two dye swaps.

GenePix ".gpr" files were processed using the limma package in Bioconductor (Gentleman et al., 2004; Smyth, 2004). Within-array loess normalization was conducted with the normexp background correction method (Ritchie et al., 2007) and an offset value of 25; the scale method was utilized for between-array normalization. Normalized values for each spot were fitted to a linear model, and moderated *t*-statistics and adjusted *p*-values were calculated for each probe on the array. For all transcripts represented by two or more unique probes, M, A, and *p*-values were averaged; a total of 3106 probes representing 1514 transcripts had M values greater than 0.6 (~1.5-fold enriched in intestinal cells) (Tables S1; Figure S1). 15 individual probes had M values greater than 1, but average M values less than 0.6; these were also included in the list of top hits. Additionally, 95 individual probes had adjusted *p*-values higher than 0.05 (a 5% false discovery rate). In 89 cases, however, the *p*-value of the alternate probe(s) representing the same transcript was lower than 0.05. Additionally, we validated intestinal expression by whole mount in situ hybridization for 8/9 transcripts with average *p*-values >0.05. For these reasons, these genes were included in the Gene Ontology annotation and, in two cases, initial RNAi experiments.

Gene ontology annotation and assignment of gene IDs

Gene ontology terms (Ashburner et al., 2000) were assigned to genes represented on the arrays using Annot8r (http://www.nematodes.org/bioinformatics/annot8r/index.shtml) (Schmid and Blaxter,

2008). Specifically, BLAST homology searches of planarian sequences were conducted against the UniProt database. GO terms annotated to the top five UniProt BLAST hits with E-values lower than 0.001 were assigned to planarian genes; “IEA” (Inferred from Electronic Annotation) terms were excluded from annotation. For the genes that yielded RNAi phenotypes (17), all annotations were assigned based on BLAST hits with E-values of e-06 or lower, and for 14/17 genes, e-values were e-10 or lower (Table S4). Furthermore, for all annotations (1597) assigned to the 100 genes we included in our RNAi screen, 1504/1597 (~94%) of GO assignments were made based on e-values of e-08 or lower, and 1568/1597 (~98%) were based on e-values of e-5 or lower. Similarly, for all 1514 intestinally enriched genes, 10,095/11,555 (~87%) annotations were made based on hits with e-values of e-08 or lower, and 11,083/11,555 (~96%) were based on e-values of e-05 or lower. Annot8r output flat files were manually formatted into the gene ontology association (.goa) file format, then mapped to custom GO Slim ontologies generated using OBO-edit (Day-Richter et al., 2007) with the “map2slim” script in GO-Perl (Camon et al., 2004).

Gene IDs were assigned to the 1514 intestine-enriched transcripts based on the top UniProtKB hit from the gene ontology annotation using Annot8r; a second set of IDs were generated based on the top BLASTX hit in the NCBI Swissprot protein database (Table S3). For genes with RNAi phenotypes, BLASTX searches were also conducted against the NCBI refseq protein database (Table S4).

For CerS1 and NKX domain alignments, homologs from various species were identified in NCBI and aligned using CLUSTALW2 at EBI (http://www.ebi.ac.uk/Tools/msa/clustalw2/) (Larkin et al., 2007; Goujon et al., 2010); shaded alignments were created using BOXSHADE (http://www.ch.embnet.org/software/BOX_form.html). For Lag1p motif alignments, domains were identified in the following proteins (NCBI Accession Numbers in

parentheses): *S. mediterranea* CerS1, MAKER prediction mk4.000148.01.01 (Robb et al., 2008); *S. cerevisiae* Lag1p (NP_011860.1); *C. elegans* HYL-1 (NP_501459.1); *D. melanogaster* schlank (AAF46137.2); *H. sapiens* LAG1 (AAD16892.1); *M. musculus* LAG1 (AAI32319.1); *H. sapiens* LASS2 (NP_859530.1); *M. musculus* LASS2 (NP_084065.1); *H. sapiens* LASS5 (NP_671723.1); *M. musculus* LASS5 (NP_082291.1). For alignment of NKX homeodomains: *S. mediterranea* NKX-2.2, Contig5669 (Zayas et al., 2005), MAKER prediction mk4.004210.02.01, and "de novo" prediction de_novo.22849.1 (Robb et al., 2008); *G. tigrina* DTH-1 (CAA39854.1); *H. sapiens* Nkx-2.2 (NP_002500.1); *M. musculus* Nkx-2.2 isoform 1 (NP_035049.1); *D. rerio* Nkx-2.2a (NP_571497.1); *X. laevis* XENK-2 (NP_001079091.1); *G. gallus* Nkx2.2 (XP_003643855.1); *C. teleta* NK-like homeobox protein 2.2b (ACH89433.1); *S. purpuratus* NK2.2 (AAS58444.1); *S. mansoni* nk-2 (XP_002581978.1); *D. melanogaster* ventral nervous system defective/NK-2B (NP_001036253.1); *C. elegans* CEH-22 (NP_001076742.1); *M. musculus* Nkx-2.1 (NP_033411.3); *M. musculus* Nkx-2.3 (AAF08008.1); *M. musculus* Nkx-2.4 (AAG35619.1); *M. musculus* Nkx-2.5 (NP_032726.1); *D. melanogaster* tinman (NP_524433.1); *M. musculus* Nkx-2.6 (AAC15674.1); *M. musculus* Nkx-3.1 (AAC52956.1).

Construction of the p2T7TA derivative dsRNA feeding vector

We cloned ESTs into a derivative of the vector "p2T7TAblue" (Alibu et al., 2005) (http://trypanofan.path.cam.ac.uk/trypanofan/vector/) optimized for dsRNA expression in *E. coli*. Standard cloning techniques were utilized to remove: the rDNA spacer/targeting fragment; the hygromycin resistance gene and *T. brucei* actin processing sequences; and the Tet operator sequences. Additionally, the "death cassette" from pPR244 (Reddien et al., 2005) was inserted into the lacZ stuffer to enable more efficient cloning. Amplified ESTs were ligated into the Eam1105I-digested vector purified using the DNA

Clean & Concentrate Kit (Zymo) as described (http://trypanofan.path.cam.ac.uk/trypanofan/protocols/).

Immunofluorescence

Animals were relaxed and killed in 0.66 M $MgCl_2$ (diluted in planarian salts) for 15-30 sec, rinsed in PBS, shaken in ice-cold 2% HCl (3 min), fixed in methacarn (15 min), rinsed in methanol (15 min), then bleached O/N in 6% H_2O_2. For proliferation analysis, animals were fixed in Carnoy's (Umesono et al., 1997). After rehydration and O/N blocking (Forsthoefel et al., 2011), animals were incubated O/N in MAb 3G9 supernatant diluted 1:3 in blocking buffer, washed over 8 h, incubated with goat anti-mouse IgG+IgM HRP (1:250, Jackson Labs), and washed again, followed by tyramide signal amplification (TSA) with FITC-tyramide (Pearson et al., 2009; Forsthoefel et al., 2011). Labeling with rabbit anti-muscle serum or rhodamine-LCA (Vector Labs) was conducted on 3G9-labeled specimens as described (Zayas et al., 2010; Forsthoefel et al., 2011). For proliferation analyses, animals were fixed in Carnoy's (Umesono et al., 1997) and incubated with mouse anti-phosphohistone-H3-Ser10 (1:25, Cell Signaling) or rabbit anti-phosphohistone-H3-Ser10 (1:500, Millipore), followed by goat anti-mouse HRP (1:100, Invitrogen) or goat anti-rabbit HRP (1:500, Jackson); FITC-tyramide (above) or Cy3-tyramide (Perkin Elmer) were utilized for detection. Quantification of H3-S10P+ cells was conducted in ImageJ (Abramoff et al., 2004).

Generation of monoclonal antibody 3G9

We conducted ~50 intestinal phagocyte collections by magnetic sorting, above, fixing half of the cells in methanol, and the other half in 4% formaldehyde/1X PBS. Balb/c female mice were injected three times (every three weeks) with ~5 x 10^5 to 10^6 cells per injection, with one boost of ~9 x 10^5 cells. Antigen emulsion was made by mixing cell suspension with a chosen adjuvant at an equal volume. Titermax adjuvant

and incomplete Freund's adjuvant were used for primary immunization and subsequent immunizations, respectively. The best immune responders to intestinal cells were sacrificed and their lymphocytes fused with Sp2/0 myeloma cells to generate hybridoma cell lines following standard protocols (Kohler and Milstein, 1975). Fusions secreting specific antibodies to target cells were subcloned to make final hybridoma cell lines. Modified standard HAT medium containing 10% FBS was used to culture hybridoma cells in a 7% CO_2 incubator. Antibody-producing lines will be submitted to the Developmental Studies Hybridoma Bank, Iowa City, IA.

Quantitative PCR

Total RNA was extracted from individual planarians using Trizol (Invitrogen) seven days after one (*CerS1/*Contig2269), two (*nkx-2.2/*Contig5669*, mob-1/*Contig1173) or three (*egfp, tpm-1/*Contig5776*, CerS1/*Contig2269*, endo-A3/*Contig1883, *DDX3/*Contig4698) dsRNA feedings. After DNAse treatment (DNAse-free RNA kit, Zymo Research), one µg RNA was used for reverse transcription (iScript cDNA synthesis kit, Biorad). 100 ng cDNA were used as the template for real-time PCR using GoTaq Master Mix (Promega) and a StepOnePlus System (Applied Biosystems) running StepOne v2.1 software. Three technical replicates were performed on each of 3-4 biological replicates; mean Ct values were normalized to the endogenous control *Smed-Ef2* (Fernandéz-Taboada et al., 2010). Resulting ΔCt values were used to calculate relative expression (RQ), averaged, and normalized to the *egfp(RNAi)* control for each knockdown/primer set. The following primers were used:

Ef2 F: 5' CAGCCAGTAGCTTTAAGCGATGA
Ef2 R: 5' ACTCTCAACGCTGCTGTCACTTC
tpm-1 F: 5' ATGCTTGCTGATGCTACGAG
tpm-1 R: 5' GCAGAACACGTTCTCACACA
CerS1 F: 5' CTGCTGATGCTGTTGTTCCT
CerS1 R: 5' TCCTCCTCCAATTCTCGAAC
nkx-2.2 F: 5' ACAACCCGAACCAGAAAGAC

nkx-2.2 R: 5’ TTACCAACATCACCCGAAGA
mob-1 F: 5’ CGATCAAGTGTTCTGCTCCT
mob-1 R: 5’ TCGTTGTCAAGCTGATCCTG
endo-A3 F: 5’ CACGACACATCACAATCCAC
endo-A3 R: 5’ CGAACCAACTGTCATCGACT
DDX3 F: 5’ GTTGGCCATCTTGGAGAATC
DDX3 R: 5’ CCTGTTGTGCCTCTTCCAAA

Transmission electron microscopy

Animals were fixed in 2% formaldehyde, 2.5% glutaraldehyde in EMBuffer (70 mM sodium cacodylate Buffer, pH 7.4 plus 1 mM $CaCl_2$) for 10 min on ice, excised, fixed further for 4 hr, washed twice in EMBuffer and post-fixed with 1% OsO_4 for 90 min; all steps at 4 °C in the dark. Samples were washed twice in EMBuffer followed by ethanol series (20% plus 2% uranyl acetate, 40%, 60%, 80%, 100%), then gradual replacement of ethanol with acetone and infiltration with Araldite/Embed 812 (Electron Microscopy Sciences). Sections (80 nm) were post-stained with lead citrate and imaged on a Hitachi H600 Transmission Electron Microscope at 75 kV. Chemicals were from Polysciences, Inc., unless noted.

BrdU labeling

egfp(RNAi) or *CerS1(RNAi)* animals were fed 2 mg/ml 5-bromo-2’-deoxyuridine (Sigma) five days after the third dsRNA feeding and cryosectioned; antigen retrieval followed by BrdU and enteric muscle detection was performed as in (Forsthoefel et al., 2011).

TUNEL

egfp(RNAi) or *nkx-2.2(RNAi)* animals were killed, fixed, and permeabilized as in (Pellettieri et al., 2010). Unbleached animals were cryoprotected and cryosectioned as for BODIPY labeling. Antigen retrieval was performed (Forsthoefel et al., 2011), followed

by permeabilization/denaturation with 2:1 ethanol/acetic acid and detection of apoptotic cells using the ApopTag Red kit (Millipore).

Supplemental References

Abramoff, M.D., Magelhaes, P.J., and Ram, S.J. (2004). Image Processing with ImageJ. Biophotonics International *11*, 36-42.

Alibu, V.P., Storm, L., Haile, S., Clayton, C., and Horn, D. (2005). A doubly inducible system for RNA interference and rapid RNAi plasmid construction in *Trypanosoma brucei*. Mol. Biochem. Parasitol. *139*, 75-82.

Ashburner, M., Ball, C.A., Blake, J.A., Botstein, D., Butler, H., Cherry, J.M., Davis, A.P., Dolinski, K., Dwight, S.S., Eppig, J.T.*, et al.* (2000). Gene ontology: tool for the unification of biology. The Gene Ontology Consortium. Nat. Genet. *25*, 25-29.

Camon, E., Magrane, M., Barrell, D., Lee, V., Dimmer, E., Maslen, J., Binns, D., Harte, N., Lopez, R., and Apweiler, R. (2004). The Gene Ontology Annotation (GOA) Database: sharing knowledge in Uniprot with Gene Ontology. Nucleic Acids Res. *32*, D262-266.

Day-Richter, J., Harris, M.A., Haendel, M., and Lewis, S. (2007). OBO-Edit--an ontology editor for biologists. Bioinformatics *23*, 2198-2200.

Fernandéz-Taboada, E., Moritz, S., Zeuschner, D., Stehling, M., Schöler, H.R., Saló, E., and Gentile, L. (2010). Smed-SmB, a member of the LSm protein superfamily, is essential for chromatoid body organization and planarian stem cell proliferation. Development *137*, 1055-1065.

Forsthoefel, D.J., Park, A.E., and Newmark, P.A. (2011). Stem cell-based growth, regeneration, and remodeling of the planarian intestine. Dev. Biol. *356*, 445-459.

Gentleman, R.C., Carey, V.J., Bates, D.M., Bolstad, B., Dettling, M., Dudoit, S., Ellis, B., Gautier, L., Ge, Y., Gentry, J.*, et al.* (2004). Bioconductor: open software development for computational biology and bioinformatics. Genome Biol. *5*, R80.

Goujon, M., McWilliam, H., Li, W., Valentin, F., Squizzato, S., Paern, J., and Lopez, R. (2010). A new bioinformatics analysis tools framework at EMBL-EBI. Nucleic Acids Res. *38*, W695-699.

Kohler, G., and Milstein, C. (1975). Continuous cultures of fused cells secreting antibody of predefined specificity. Nature *256*, 495-497.

Larkin, M.A., Blackshields, G., Brown, N.P., Chenna, R., McGettigan, P.A., McWilliam, H., Valentin, F., Wallace, I.M., Wilm, A., Lopez, R.*, et al.* (2007). Clustal W and Clustal X version 2.0. Bioinformatics *23*, 2947-2948.

Pearson, B.J., Eisenhoffer, G.T., Gurley, K.A., Rink, J.C., Miller, D.E., and Sánchez Alvarado, A. (2009). Formaldehyde-based whole-mount in situ hybridization method for planarians. Dev. Dyn. *238*, 443-450.

Pellettieri, J., Fitzgerald, P., Watanabe, S., Mancuso, J., Green, D.R., and Sánchez Alvarado, A. (2010). Cell death and tissue remodeling in planarian regeneration. Dev. Biol. *338*, 76-85.

Reddien, P.W., Bermange, A.L., Murfitt, K.J., Jennings, J.R., and Sánchez Alvarado, A. (2005). Identification of genes needed for regeneration, stem cell function, and tissue homeostasis by systematic gene perturbation in planaria. Dev. Cell *8*, 635-649.

Ritchie, M.E., Silver, J., Oshlack, A., Holmes, M., Diyagama, D., Holloway, A., and Smyth, G.K. (2007). A comparison of background correction methods for two-colour microarrays. Bioinformatics *23*, 2700-2707.

Robb, S.M., Ross, E., and Sánchez Alvarado, A. (2008). SmedGD: the *Schmidtea mediterranea* genome database. Nucleic Acids Res *36*, D599-606.

Schmid, R., and Blaxter, M.L. (2008). annot8r: GO, EC and KEGG annotation of EST datasets. BMC Bioinformatics *9*, 180.

Smyth, G.K. (2004). Linear models and empirical bayes methods for assessing differential expression in microarray experiments. Stat. Appl. Genet. Mol. Biol. *3*, Article 3.

Spassieva, S., Seo, J.G., Jiang, J.C., Bielawski, J., Alvarez-Vasquez, F., Jazwinski, S.M., Hannun, Y.A., and Obeid, L.M. (2006). Necessary role for the Lag1p motif in (dihydro)ceramide synthase activity. J. Biol. Chem. *281*, 33931-33938.

Umesono, Y., Watanabe, K., and Agata, K. (1997). A planarian *orthopedia* homolog is specifically expressed in the branch region of both the mature and regenerating brain. Dev. Growth Differ. *39*, 723-727.

Zayas, R.M., Cebrià, F., Guo, T., Feng, J., and Newmark, P.A. (2010). The use of lectins as markers for differentiated secretory cells in planarians. Dev. Dyn. *239*, 2888-2897.

Zayas, R.M., Hernandez, A., Habermann, B., Wang, Y., Stary, J.M., and Newmark, P.A. (2005). The planarian *Schmidtea mediterranea* as a model for epigenetic germ cell specification: analysis of ESTs from the hermaphroditic strain. Proc. Natl. Acad. Sci. USA *102*, 18491-18496.